

# Scatter in nonlinear ultrasonic measurements due to crystallographic orientation change induced anisotropy in harmonics generation

Amretendu Mukhopadhyay<sup>1</sup>, Rajdeep Sarkar, Sony Punnose, Jitendra Valluri, T. K. Nandy, and Krishnan Balasubramaniam

Citation: *J. Appl. Phys.* **111**, 054905 (2012); doi: 10.1063/1.3686698

View online: <http://dx.doi.org/10.1063/1.3686698>

View Table of Contents: <http://aip.scitation.org/toc/jap/111/5>

Published by the [American Institute of Physics](#)

---

---

## Scatter in nonlinear ultrasonic measurements due to crystallographic orientation change induced anisotropy in harmonics generation

Amretendu Mukhopadhyay,<sup>1,a)</sup> Rajdeep Sarkar,<sup>1</sup> Sony Punnose,<sup>1</sup> Jitendra Valluri,<sup>2</sup> T. K. Nandy,<sup>1</sup> and Krishnan Balasubramaniam<sup>2</sup>

<sup>1</sup>Defence Metallurgical Research Laboratory, Kanchanbagh, Hyderabad-500058, India

<sup>2</sup>Centre for Nondestructive Evaluation, Indian Institute of Technology, Chennai-600036, India

(Received 1 May 2011; accepted 26 January 2012; published online 2 March 2012)

Present study endeavors to establish the physical basis of an unprecedented trend in scatter, observed in nonlinear ultrasonic (NLU) parameter, associated with varying degree of crystallographic orientation change across crystallites in a polycrystalline material. It is shown that this scatter arises due to anisotropy in harmonics generation as a result of orientation change of slip systems in polycrystals with respect to the wave propagation direction. A near  $\alpha$  titanium alloy has been taken as a model alloy to demonstrate this effect of crystallographic orientation change vis-à-vis change in the orientation of slip systems. Scale of crystal orientation change is shown to have a strong correlation with the degree of scatter in NLU measurements. Further, the study establishes the dominating effect of the scale of crystalline orientation change on harmonics generation as compared to variation in other microstructural parameters such as dislocation density, interface structure etc. Frequency distribution analysis of the scatter indicates that the distribution depends on the colony size which exhibits a linear correlation with standard deviation value. The dislocation string vibration model has been extended for harmonics generation in polycrystalline aggregates to explain the trend in the scatter during measurement of NLU parameter in the material. © 2012 American Institute of Physics. [doi:10.1063/1.3686698]

### I. INTRODUCTION

Sinusoidal ultrasonic wave of a particular frequency gets progressively distorted while propagating through a material in the presence of various possible sources of nonlinearity. Different parts of the wave travels with different phase velocities causing a change in the shape of the particle velocity waveform which is characterized by the growth of harmonics. In early studies, the phenomenon of harmonics generation was employed as a technique mainly for the determination of the higher order elastic constants of crystals.<sup>1,2</sup> Of late, the technique is also being used to characterize different microstructural changes that are associated with viz., changes in carbon content in martensitic steel,<sup>3</sup> volume fraction of second phase precipitates,<sup>4</sup> etc. Owing to the significantly enhanced sensitivity, the nonlinear ultrasonic (NLU) technique has also been used to study the precipitation hardening kinetics in aluminum alloys,<sup>5,6</sup> the fatigue damage studies in structural materials,<sup>7-9</sup> and creep damage studies,<sup>10-12</sup> etc. Thus, NLU technique has emerged as an important tool for detailed characterization of microstructural evolution during processing and for assessment of microstructural degradation due to in-service damages. However, one of the major issues associated with NLU study is the repeatability of measurements that appear as considerable amount of scatter in the data. It has been generally believed that the scatter in the measurements mainly comes from the uncertainties due to variation in couplant thickness, the coupling coefficient between the transducers and sample,

and electronic noises. A method to minimize the effect of couplant for better repeatability of the measurements has been reported.<sup>13</sup> The present study, in an attempt to address the reason behind the scatter in NLU measurements, conclusively establishes that a large part in the scatter originates due to the variation in microstructure. The scale of crystallographic orientation change in the materials is shown to have a strong correlation with the large scatter in NLU measurements.

The aim of the present study is to (1) highlight the effect of the degree of crystallographic orientation change in polycrystalline materials on NLU measurements, (2) understand the phenomenon of harmonics generation in polycrystalline material with such microscopic in-homogeneities/texture that develops during processing, and (3) apply this understanding for interpretation of microstructural evolution during processing.

### II. MICROSTRUCTURAL FEATURES

A  $\beta$  heat treated near  $\alpha$  titanium alloy of composition (wt. %) (Ti-5.5Al-4Sn-4Zr-0.3Mo-1Nb-0.5Si-0.06 C) has been used as a model alloy system to demonstrate the effect of microstructural in-homogeneities in the form of crystallographic orientation change, on the scatter in NLU measurements. Titanium alloys (near- $\alpha$  and  $\alpha$ - $\beta$  titanium) are subjected to two types of heat treatment:  $\alpha$ - $\beta$  and  $\beta$  heat treatment. Choice of the heat treatment is governed by the application which, in turn, decides the target mechanical properties.  $\beta$  heat treatment is a common practice for a variety of titanium alloys especially for elevated temperature

<sup>a)</sup>Author to whom correspondence should be addressed. Electronic mail: amritendu@dmrl.drdo.in.

applications. In  $\beta$  heat treatment condition, microstructure is strongly dependent on the cooling rate from the solution treatment temperature. Upon cooling from solution treatment temperature above  $\beta$  transus,  $\alpha$  phase forms in the prior  $\beta$  grain either through nucleation and growth or martensitically, depending upon the cooling rate. While slower cooling rate gives a colony type structure, faster cooling rate results in fine acicular  $\alpha$  structure. Formation of  $\alpha$  lath from the parent  $\beta$  matrix is associated with Burger orientation relationship (OR)<sup>14,15</sup> that is as follows:

$$\{0001\}_{\alpha} // \{110\}_{\beta} \text{ and } \langle 11\bar{2}0 \rangle_{\alpha} // \langle 1\bar{1}1 \rangle_{\beta}$$

Laths with parallel basal plane share the same  $\{011\}$  plane. As only two  $\langle 111 \rangle$  directions are possible in each  $\{011\}$  plane, growth direction of any lath in one  $\{011\}$  plane must correspond to the two variants of Burger OR. Owing to this OR growth of the laths in one  $\{011\}$  plane is parallel to either of the two invariant lines as shown in Fig. 1. Angle between the invariant lines is the angle between the geometric growth directions and governs the morphology of the structure. In case of furnace cooled colony structure  $\alpha$  laths within a colony grows as a single variant. With increase in cooling rate colony size decreases. Tendency to form differently oriented colonies within a prior beta grain also increases with increase in cooling. Morphology changes from aligned lath colony to fine acicular  $\alpha$  structure. Growth directions and crystallographic orientation changes randomly over small length scale.

### III. EXPERIMENTAL

#### A. Heat treatment and specimen preparation

Five specimens of the near  $\alpha$  titanium alloy have been solution annealed in  $\beta$  phase field at 1070 °C ( $\sim 20$  °C above beta transus) for 2 h followed by cooling at different rates (Table I). All the specimens were subsequently aged at 700 °C for 2 h followed by air cooling. Surface grinding of the specimens has been carried out to obtain specimens with thickness of  $(10 \pm 0.5)$  mm ensuring plane parallelism better than  $10 \mu\text{m}$ . Specimens for optical and scanning electron

TABLE I. Details of specimens with cooling rate.

Specimen ID.	Specimen	Cooling rate °C/sec	Colony Size ( $\mu\text{m}$ )
a)	Slow furnace cooling	0.016	$200 \pm 50$
b)	Fast furnace cooling	0.10	$150 \pm 50$
c)	Air cooling	6.03	$30 \pm 10$
d)	Oil quenching	67.35	$5 \pm 10$
e)	Water quenching	184.42	$0.4 \pm 0.2$

micrograph have been prepared by conventional metallographic techniques and etched with Kroll's reagent. Specimens for transmission electron microscopy (TEM) has been prepared using Fichione jet polisher using 5%  $\text{H}_2\text{SO}_4$  solution at  $-50$  °C at 12 V. FEI TECNAI 20 T TEM at 200 kV has been used to study changes in dislocation density, the morphology of the second phases.

#### B. Measurements of ultrasonic parameter

A RITEC SNAP RAM-5000 high power ultrasonic system was used for ultrasonic measurements. A computer controlled transmitter-receiver capable of generating sinusoidal waveforms (in the tone-burst mode) with selectable number of cycles was used to drive the transducers. The RITEC system that is fully computer controlled contains two gated amplifiers of different frequency ranges, a super-heterodyne receiver which is capable of filtering, reversing phase and frequency sweeping of fundamental, second and third harmonics. The system incorporates an RF gated amplifier module to deliver very high power RF tone bursts that are needed for extracting higher harmonics and also for generating numerous cycles of long bursts especially suitable for materials with high attenuation characteristics. The experimental setup is shown in Fig. 2. An RF tone burst of a certain frequency and pulse width is transmitted into the material under study, and the "distorted" signal is recorded in the transmission mode. Specimens are insonified at a fundamental frequency of 10 MHz and second harmonics along with the fundamental signal is received by a high power 20 MHz Lithium Niobate transducer. By varying the input excitation

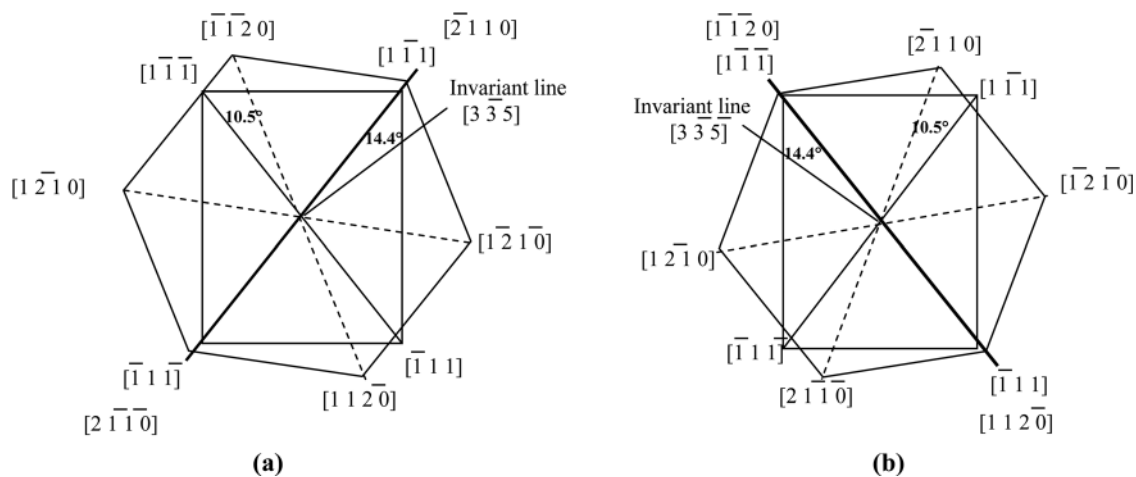


FIG. 1. Schematic of Burgers orientation relationship (a) variant 1 (b) variant 2.

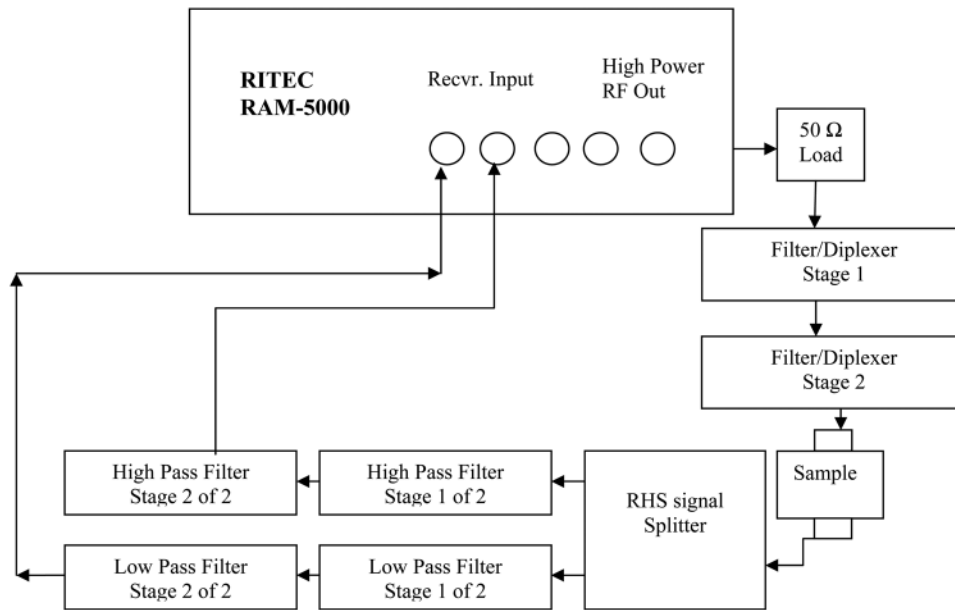


FIG. 2. Block diagram of the experimental setup for measuring nonlinear ultrasonic parameter.

voltage, a series of fundamental ( $A_1$ ) amplitudes are generated and the corresponding second harmonics ( $A_2$ ) amplitudes are recorded. Slope of  $A_2$  versus  $A_1^2$  plot are measured for series of  $A_1$  values and linear correlation is obtained. Using the value of slope, second harmonics based NLU parameter which is a material dependent property is computed using the following relationships

$$\beta' = \frac{8v^2 A_2}{\omega^2 z A_1^2}, \quad (1)$$

where  $\beta'$  = second harmonics based nonlinear parameter,  $v$  = longitudinal velocity,  $z$  = thickness of specimen,  $\omega$  is the fundamental frequency. Since the amplitude of fundamental and higher order harmonics are measured in terms of mV (not displacement), the nonlinear parameter  $\beta'$  is function of  $A_2/A_1^2$  is relative term having unit of 1/mV. Experimental error due to the noise from the system was determined to be less than  $\pm 1\%$ . Value thus obtained is further normalized with respect to the  $\beta'$  value of air cooled specimens in order to reduce the systematic error of the instrument. Measurements were repeated several times at different locations. It is noted that range of variation for the values measured in the experiments is large and is highest in case of the slow furnace cooled structure and gradually decreases with increasing cooling rate. In order to understand the scatter behavior in detail, frequency distribution analysis was carried out for about 100 measurements for  $\beta'$  parameter at different locations in slow furnace cooled, air cooled and water quenched specimens. Measurements were also repeated 10 times for  $\beta'$  parameter for a given location of a specimen with fixed orientation in each case of slow furnace cooled, air cooled and water quenched specimens.

Ultrasonic longitudinal phase velocity was measured in pulse echo mode using a 200 MHz pulser receiver (Olympus NDT Panametrics PR5900) with a 20 MHz transducer of 3 mm diameter. The signal was digitized at 1 Gs/s rate using an Analog to Digital converter card. For each specimen

10 measurements were done and average of the 10 measurements was taken for comparison.

## IV. RESULTS

### A. Nonlinear ultrasonic parameter

Figure 3 shows plot of normalized relative NLU parameter  $\beta'$  versus cooling rate. Considerable variations are observed in the values of  $\beta'$  measured at different locations of specimens and are manifested in significant scatter. An overall trend can be seen when mean values ( $\sim 11\%$  change in mean value) are considered; however, this trend is almost eclipsed by the predominant scatter in the measured values. Further, it is observed that scatter in the values of NLU parameter is the maximum in the furnace cooled specimen and gradually decreases with increasing cooling rate. Frequency distribution analysis for  $\beta'$  parameter at different locations in each case of slow furnace cooled, air cooled and water quenched specimens show an interesting pattern in the distribution. Results that are composed of mean, standard

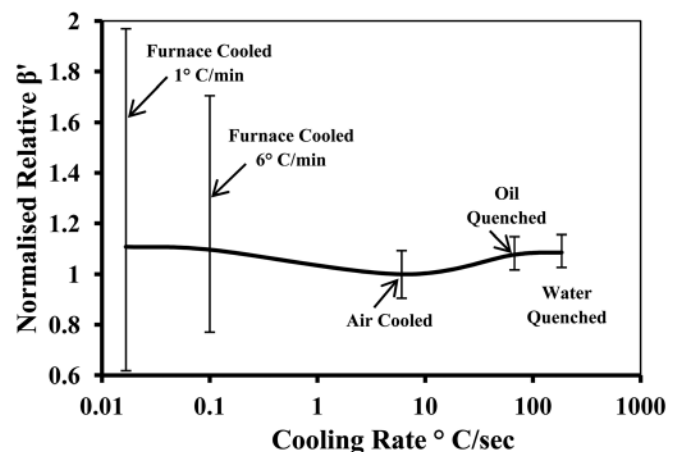


FIG. 3. Variation in normalized relative  $\beta'$  with cooling rate.

TABLE II. Analysis of around 100 NLU measurements done on three specimens.

Specimen	Mean	Median	Standard Deviation	Skew $\left(\frac{1/n \sum_{i=1}^n (x_i - \bar{x})^3}{(1/n \sum_{i=1}^n (x_i - \bar{x})^2)^{3/2}}\right)$
Furnace cooled	$8.94 \times 10^{-4}$	$8.75 \times 10^{-4}$	$1.89 \times 10^{-4}$	1.129
Air cooled	$8.06 \times 10^{-4}$	$8.09 \times 10^{-4}$	$4.33 \times 10^{-5}$	$-1.512 \times 10^{-01}$
Water Quenched	$8.76 \times 10^{-4}$	$8.76 \times 10^{-4}$	$2.46 \times 10^{-5}$	$-2.813 \times 10^{-03}$

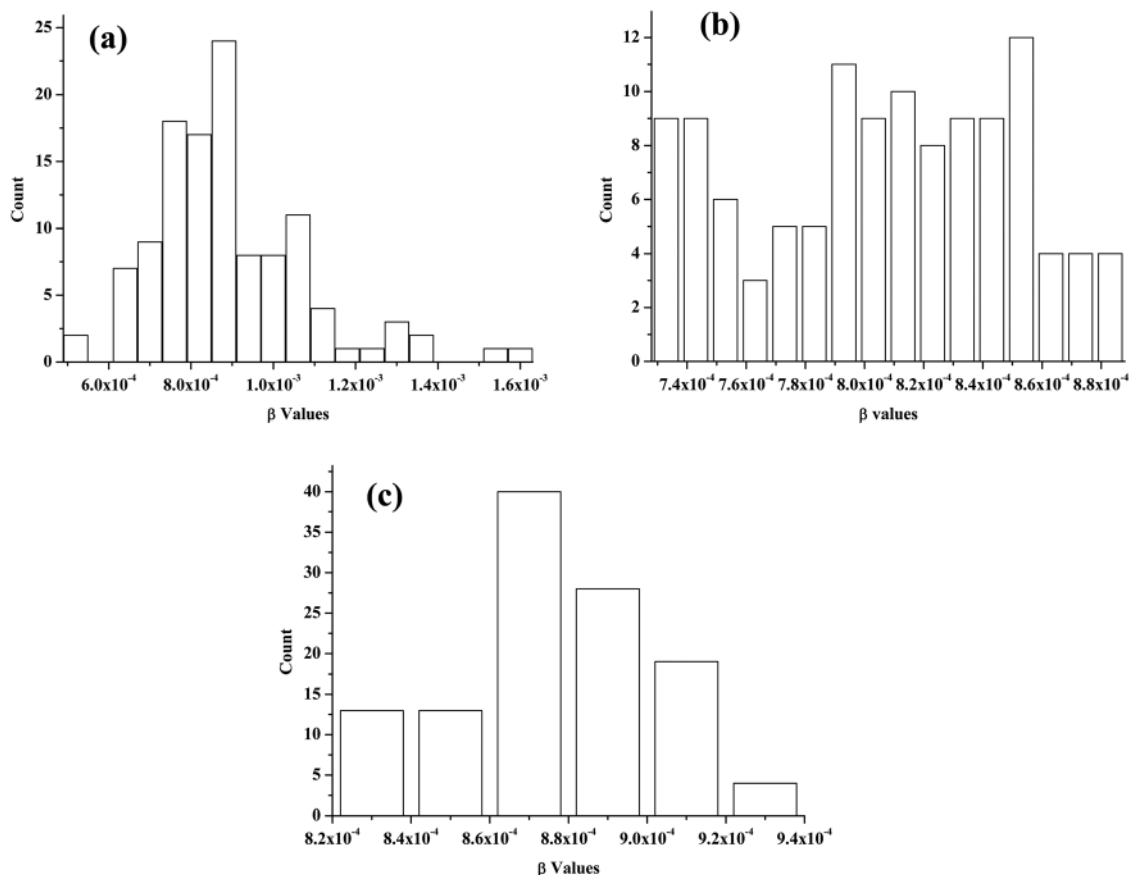
deviation, median value and the skew of distribution for the three specimens are shown in Table II. Corresponding plots are shown in Fig. 4(a)–4(c). For the slow furnace cooled specimen, the standard deviation is highest with distribution being positively skewed. With increase in the cooling rate the standard deviation value decreases and distributions become symmetric. Figure 5 shows plot of standard deviation and colony size versus cooling rate in slow furnace cooled, air cooled and water quenched specimen which shows as cooling rate decreases both standard deviation and colony size decreases. Corresponding plot (Fig. 6) of colony size versus standard deviation shows that good linear correlation exists between colony size and standard deviation values. It is to be noted that in water quenched structure the colony size is almost equal to the size of  $\alpha$  laths and thus thickness of  $\alpha$  lath is taken as a measurement of colony size in case of water quenched structure. Table III shows the mean, median and standard deviation values obtained in the case of the measurements done at fixed orientation and loca-

tion for the three specimens. It can be noticed that standard deviation values are almost equal.

Ultrasonic longitudinal phase velocity shows a reverse trend as shown in Fig. 7, though the dependence is only marginal (3% change in phase velocity).

## B. Micro-structural characterization

Detailed microstructural characterization has been carried out to understand the typical trend in the scatter vis-à-vis scale of variation in microstructural features with cooling rate. Optical, scanning electron secondary images of transformed  $\beta$  structure as a function of cooling rate are shown in Fig. 8 and Fig. 9 respectively. They clearly show that the microstructure is sensitively dependent on cooling rate. In furnace cooled structure, microstructure comprises similarly aligned  $\alpha$  laths forming  $\alpha$  colonies within the prior  $\beta$  grains. With increasing cooling rate, the thickness of  $\alpha$  laths and the size of  $\alpha$  colony decreases. Tendency to form differently

FIG. 4. Frequency distribution of  $\beta'$  values obtained for (a) furnace cooled at  $1^\circ\text{C}/\text{min}$ , (b) air cooled, and (c) water quenched specimen.

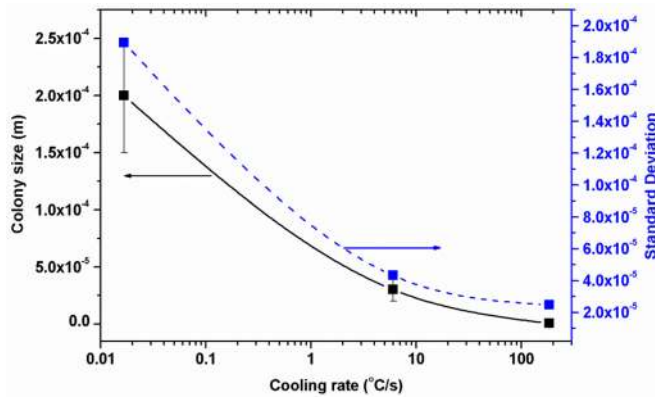


FIG. 5. (Color online) Variation in colony size vis-à-vis standard deviation with cooling rate.

oriented colonies within a prior beta grain also increases with cooling rate. The colony structure degenerates into randomly oriented  $\alpha$  platelets especially in oil and water quenched specimens, the thickness of  $\alpha$  platelets is lowest in water quenched structure. Selected area diffraction pattern (SADP) of  $\alpha$  lath is shown in Fig. 10, presence of super lattice spots points toward  $\alpha_2$  phase which is present in all specimens. The details of retained  $\beta$  film can only be seen by transmission electron microscopy (Figs. 11 and 12). In furnace cooled and air cooled specimens the film is continuous whereas in the oil quenched specimen, the film is discontinuous and broken at several places. In water quenched specimen,  $\beta$  film is almost absent (Fig. 12). Figure 13 shows dislocation substructure in the vicinity of  $\alpha$ - $\beta$  interface. A high dislocation density near the walls is observed in both air cooled and oil quenched specimen. Dislocation substructure inside the  $\alpha$  lath interior for different cooling rates is shown in Fig. 14. Presence of both large and short segments of dislocation depending upon the orientation of foil (with respect to  $\alpha$ ) is seen. Examination of numerous areas of the foil within the specimens suggests that the dislocation density increases with increasing cooling rate.

## V. DISCUSSION

Figure 3 shows that scatter in the measured values is dominant over the average trend. Though the scatter in measurement is large but interestingly it shows a trend. As the ex-

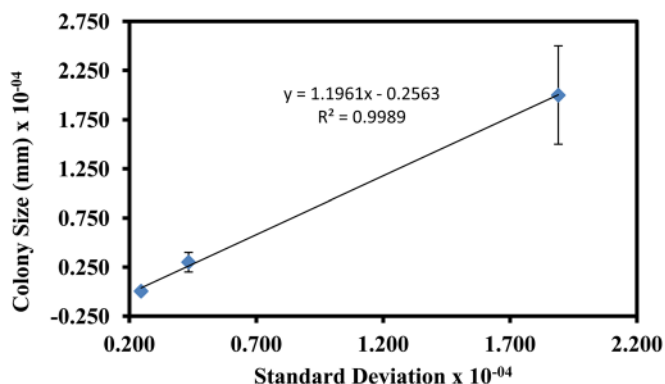


FIG. 6. (Color online) Variation in colony size with standard deviation of measurements.

TABLE III. Analysis of 10 measurements done on three specimens at the same location and orientation.

Specimen	Mean	Median	Standard Deviation
Furnace cooled	$6.63 \times 10^{-04}$	$6.56 \times 10^{-04}$	$2.64 \times 10^{-05}$
Air cooled	$8.44 \times 10^{-04}$	$8.45 \times 10^{-04}$	$4.28 \times 10^{-05}$
Water Quenched	$8.96 \times 10^{-04}$	$8.91 \times 10^{-04}$	$1.98 \times 10^{-05}$

perimental conditions were kept similar in all the measurements, a gradual decrease in the standard deviation suggests that the large scatter inherently come from variation in microstructural features with cooling rate. Nearly equal values of standard deviation obtained in measurements done on the three specimens at fixed orientation and location (Table III) further indicate that the observed scatter originates from the change in locations and orientations of the specimens during measurements. Changes in the location and orientations of specimens during measurements can cause change in crystallographic orientations of the grains with respect to the wave propagation directions. This can lead to recording of different values of  $\beta'$  during measurements for a given specimen. Thus, to clearly understand the source of scatter in the present alloy, harmonics generation has been studied from the viewpoint of wave-material interaction in the polycrystalline material with varying scale of microstructural features. The wave equation describing a pure longitudinal wave propagating in certain special (arbitrary) direction in an anisotropic nonlinear medium can be written as<sup>16</sup>

$$\frac{\partial^2 u}{\partial t^2} = g \left( \frac{\partial u}{\partial x} \right) \frac{\partial^2 u}{\partial x^2}, \quad (2)$$

where  $x$  is the propagation direction and  $u$  is the particle displacement.

The shape of the distorted wave form and the associated shift of energy to various harmonics depend on the explicit form of the function  $g \left( \frac{\partial u}{\partial x} \right)$ . For most solids, the sign of the derivative  $g' \left( \frac{\partial u}{\partial x} \right)$  is negative and leads to forward sloping wave form. In their pioneering work, Hikata *et al.*,<sup>17</sup> has shown that the functional form of  $g \left( \frac{\partial u}{\partial x} \right)$  has two contributing nonlinear factors. One is the lattice anharmonicity and the other due to the nonlinear part of the stress-strain relationship for any dislocation displacement. Considering the higher order terms in the displacement of dislocation

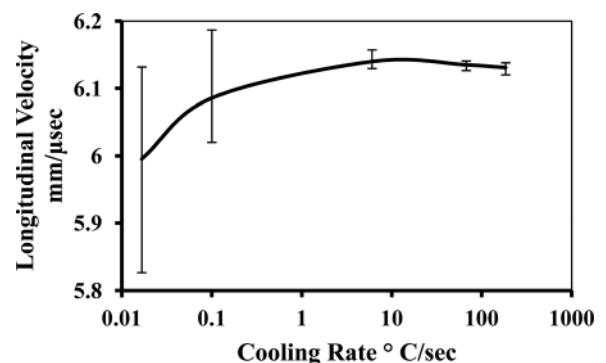


FIG. 7. Variation in longitudinal phase velocity with cooling rate.

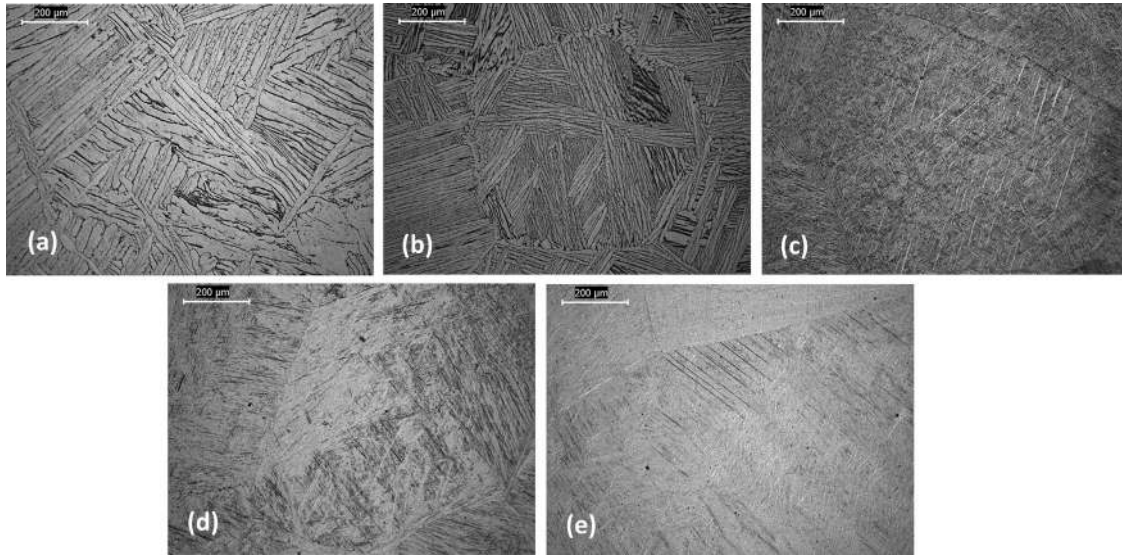


FIG. 8. Optical micrograph of specimens solution annealed at 1070 °C followed by (a) furnace cooling at 1 °C/min, (b) furnace cooling at 6 °C/min, (c) air cooling, (d) oil quenching, and (e) water quenching and subsequently aged at 700 °C followed by air cooling.

(bowing) between the pinning points and the variation in line energy along dislocations, in the dislocation string vibration model described by Granato and Lucke,<sup>18</sup> Hikata *et al.*<sup>17</sup> have shown that nonlinear relation between a static stress and the dislocation displacement leads to the following equation of motion of a dislocation under the influence of combined static and oscillatory stresses

$$A \frac{\partial^2 \xi}{\partial t^2} + B \frac{\partial \xi}{\partial t} - C \left[ \left( \frac{\partial^2 \xi}{\partial \eta^2} \right) - C' \left( \frac{\partial \xi}{\partial \eta} \right)^2 \left( \frac{\partial^2 \xi}{\partial \eta^2} \right) \right] = bR\sigma, \quad (3)$$

where  $\sigma$  is the combination of static and oscillatory stress due to ultrasonic wave,  $B$  damping coefficient of dislocation motion, and  $A$  is the effective mass of dislocation per unit length,  $R$  is the Schmid factor,  $b$  is Burgers vector,

$$C = W_e (1 + m \cos^2 \theta - 2m \sin^2 \theta), C' = \frac{3(1 + 3m \cos^2 \theta - 4m \sin^2 \theta)}{2(1 + \cos^2 \theta - 2m \sin^2 \theta)}, \quad (4)$$

wherein  $m = (W_e - W_s)/W_e$ ,  $W_e$  and  $W_s$  are line energy of edge and screw dislocation per unit length respectively,  $\theta$  is the angle between Burgers vector and the dislocation line under zero stress.

From the above relationship they have shown that in a single crystal, contribution of lattice anharmonicity toward the harmonics generation is a function of Huang elastic coefficients, which in turn can be written as linear combinations of Brugger elastic constants. On the other hand, the harmonics generation due to nonlinear dislocation motion is function of dislocation density, dislocation loop length and orientation, bias stress, etc.

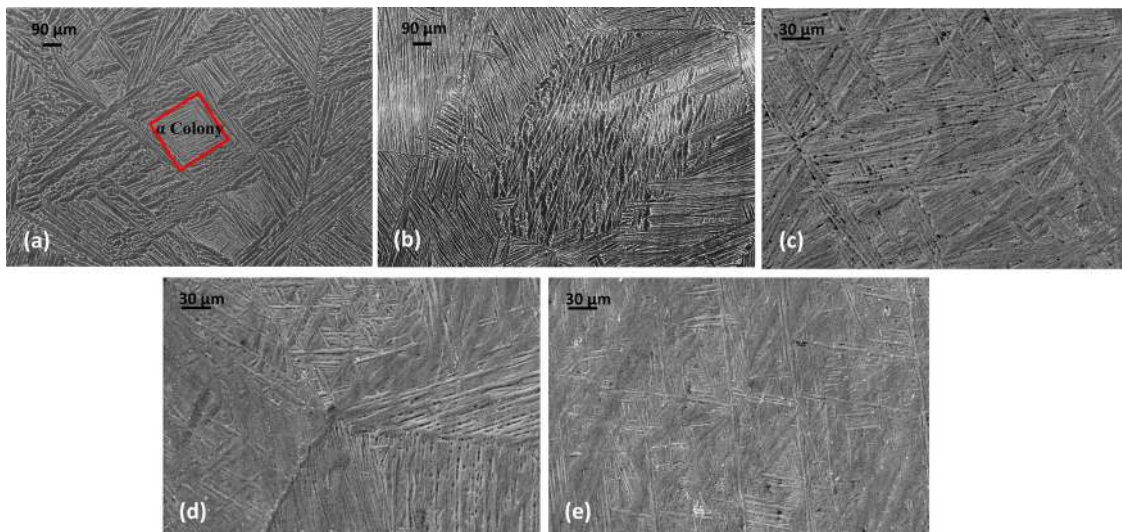


FIG. 9. (Color online) Scanning electron micrograph showing variation in morphology of  $\alpha$  lath in (a) furnace cooled at 1 °C/min, (b) furnace cooled at 6 °C/min, (c) air cooled, (d) oil quenched, and (e) water quenched specimens.

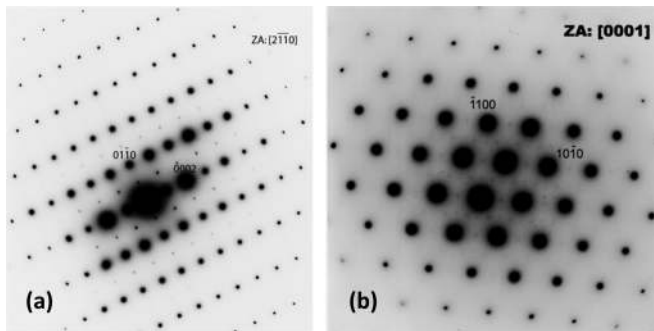


FIG. 10. Selected area diffraction patterns showing super lattice spot in (a) furnace cooled at 1 °C/min and (b) oil quenched structures.

Considering the effect of Peierls-Nabarro barrier stress on the nonlinear dynamics of dislocation motion Yost and Cantrell,<sup>19,20</sup> in a pioneering work, first pointed out that harmonics generation in polycrystalline solids depends on the randomness in orientation of the grain aggregates in addition to the contribution from each grain (crystallites). The study highlights the effect of lattice periodicity on the period of Bessel function oscillation at low stress amplitude. It has been shown that the nonlinearity parameter exhibits a Bessel function oscillatory dependence on the stress amplitude. At large amplitudes the oscillatory dependence of nonlinearity parameter diminishes and in the limiting case only static contribution from dislocation remains. Though in a different context but the study first highlights the effect of randomness of grain orientation on harmonics generation in polycrystalline solids. In the present case also the harmonics generation depends upon the nature of grain aggregation along the wave propagation path. This is due to the fact that harmonics generation is a cumulative process and in a polycrystalline solid the contribution of each grain toward harmonics generation depends upon two major factors, viz., amplitude of resolved stress on slip systems and the number of active slip systems. Both the factors, in turn, depend upon the orientation of the grain with respect to wave propagation direction, i.e., on the value of  $R$ . Thus, the nonlinearity parameter varies as function of  $R$  for different wave propagation directions. In addition to the contribution of each grain toward the amplitude of overall harmonics generation, there are different rays that travel through slightly different propagation path and get integrated at vari-

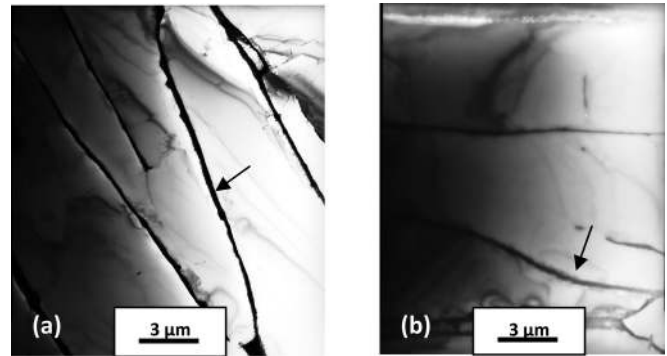


FIG. 11. Transmission electron images showing continuous layer of  $\beta$  between the  $\alpha$  laths in (a) Furnace cooled at 1 °C/min, and (b) Furnace cooled at 6 °C/min specimens.

ous points on the receiving transducer. Each such ray of acoustic waves propagate through a different series of contiguous grains and each series of contiguous grains lead to slightly different propagation path because of differences in the average grain orientation and size along the wave path. The differences in the propagation path lead to differences in phase at various points on the receiving transducer. When the different rays are integrated over the receiving transducer the measured fundamental and harmonic amplitudes vary in accordance with the phase variations from the different paths. In case of coherent interference of different rays harmonics generation will be high. Hence, in polycrystals the overall harmonics generation will depend upon factors such as (1) the integrated value of the amplitude of harmonics generated from each grain across the propagation path for a given ray, (this depends upon the integrated value of  $R$  over all the grains for a given ray), and (2) vector sum of the rays over all the slightly different paths for different rays that arrive at various points on the receiving transducer. Thus, depending upon the grain orientation vis-à-vis the direction of wave propagation harmonics generation will vary.

In polycrystalline solids there can be two cases (1) presence of preferred grain orientation (texture) and (2) perfectly random grain orientation.

(1) Presence of preferred grain orientation (texture): For this material, depending upon the orientation of specimen, further there can be two possibilities.

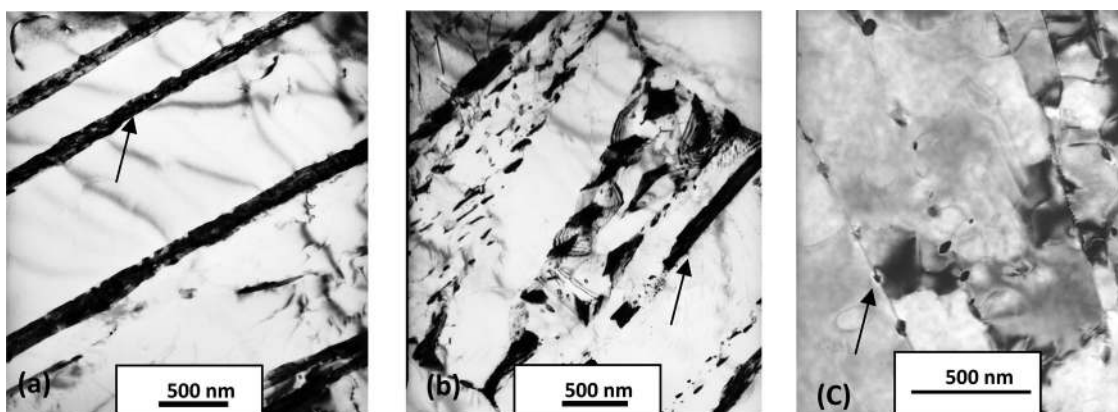


FIG. 12. Transmission electron images showing  $\beta$  between the  $\alpha$  laths in (a) air cooled, (b) oil quenched, and (c) water quenched specimens.

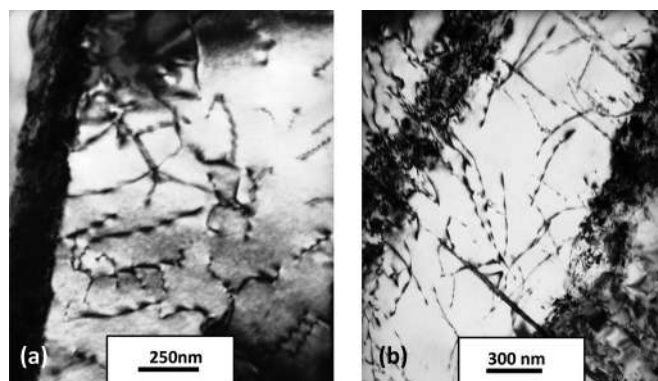


FIG. 13. Transmission electron images showing boundary between  $\alpha'$  and retained  $\beta$  consists of walls of high dislocation density in (a) air cooled, and (b) oil quenched specimens.

(a) Wave propagation along the highly symmetric crystallographic direction

Wave propagation along the highly symmetric crystal direction gives rise to simultaneous activation of several favorably oriented slip systems (with constant Schmidt factor  $R$ ) in individual crystallites (grains). Dislocation motion in all the active slip systems will contribute coherently toward harmonics generation. This is because regular/symmetric orientation of slip system ensures constant path difference vis-à-vis constant phase difference between different rays.

Hence, in case of a highly textured material where several crystallites may be favorably oriented to the high symmetric wave propagation direction, it can be envisioned that amplitude of harmonics will be very large.

(b) Wave propagation along any other directions.

For wave propagation along any general direction (other than high symmetric ones), there will be at least one slip system that will be activated and will contribute toward harmonics generation. The value of  $R$  for slip system in one crystallite will remain constant for all crystallites with similar orientation across the wave propagation direction. This will lead to dislocation displacements in the same slip system in large number of crystallites along wave propagation direction and will increase the amplitude of harmonics produced. In this case the amplitude of harmonics generated will be not as high as the one produced when the wave propagation is along the symmetric direction.

(2) Perfectly random grain orientation.

For these materials, random grain orientation leads to random orientation of slip system with respect to the wave propagation direction, hence, different slip systems will be activated across crystallites. Schmidt factor  $R$  can have any value between 0 and 0.5 for each slip system and phase relation among different rays will also be random. Randomness in the orientations of slip systems can lead to incoherent interference of different rays propagating through the material. This will reduce the amplitude of harmonics generated. It is

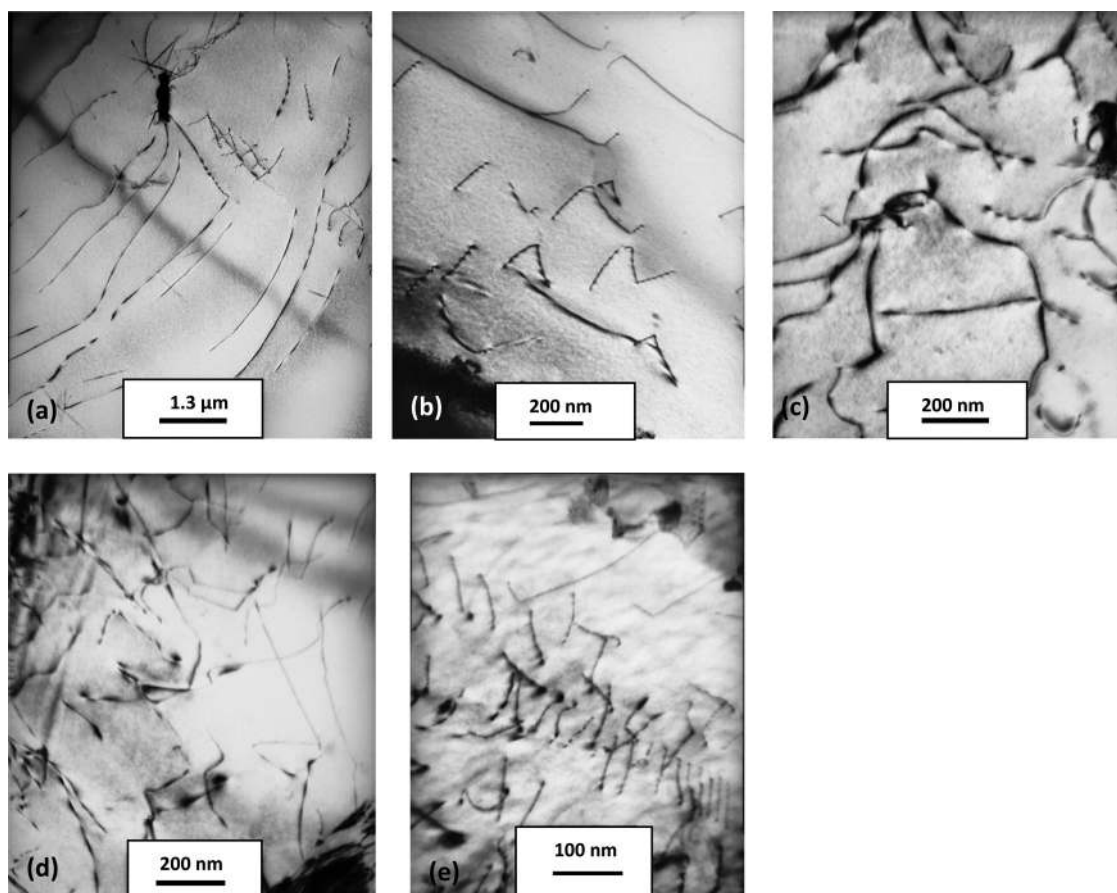


FIG. 14. Transmission electron images showing dislocations in internal regions of  $\alpha$  lath in (a) furnace cooled at  $1^\circ\text{C}/\text{min}$ , (b) furnace cooled at  $6^\circ\text{C}/\text{min}$ , (c) air cooled, (d) oil quenched, and (e) water quenched specimens.

to be noted here that because of the random grain orientation all the wave propagation directions will be almost equivalent and anisotropy in harmonics generation will be also less.

Thus, in polycrystals, apart from the other microstructural parameters, nature of grains aggregation plays an important role in the process of harmonics generation. In the present alloy to understand the effect of grain aggregation, exact nature of crystallographic orientation change of different laths/colony aggregation has been studied. Apart from this effect, the presence of fine layer of stable  $\beta$  in between the laths, the contribution of the individual lath (in terms of displacement of dislocation in individual lath, dislocation density inside lath, etc.), the interface dislocations toward harmonics generation, have been investigated to figure out the dominant microstructural feature affecting harmonics generation.

### A. Crystallographic orientation of laths/colony

One of the most important parameter that can influence harmonics generation significantly in the present alloy is the orientation of lath/colony inside prior  $\beta$  grain, orientation of prior  $\beta$  grain with respect to the wave propagation direction. Formation of  $\alpha$  lath from the parent  $\beta$  matrix is associated with Burger orientation relationship (as discussed in Sec. I). This leads to 12 variants of  $\alpha$  phase. While furnace cooling gives rise to colony structure in which laths within the colony grows as single variant (i.e., crystallographic orientation remains almost same), oil or water quenching yield nearly random structure of  $\alpha$ . Thus, it is evident that in a colony structure, all the laths in a colony will contribute toward harmonics generation and will give rise to overall increase in amplitude of harmonics produced. Depending upon the wave propagation direction vis-à-vis the colony orientation amplitude of overall harmonics generation will vary. As the cooling rate increases colony size decreases and laths become finer, different slip systems will get activated in differently oriented  $\alpha$  laths along wave propagation direction. This can lead to incoherency in harmonics generation and amplitude of harmonics generated will decrease as well as anisotropy in harmonics generation will reduce.

### B. Effect of presence of stable $\beta$ in between laths

With the increase in cooling rate fine layer of  $\beta$  that forms in between the laths become more and more discontinuous and this layer is almost absent in case of water quenched specimen. Presence of thin layer of  $\beta$  phase between the laths leads to anisotropy in the dislocation displacement. This anisotropy can be derived from the near OR that exists between the  $\alpha$  and  $\beta$  laths. Orientation of laths with respect to the wave propagation direction decides slip system will contribute significantly toward harmonics generation. Previous studies indicate that three different a-type ( $-1/3 \langle 11\bar{2}0 \rangle$ ) slip systems can be active inside the  $\alpha$  laths in near alpha titanium alloys.<sup>21</sup> Their alignment with respect to the  $\beta$  laths is shown in Fig. 15. It can be clearly seen that the  $a_1$  slip direction in  $\alpha$  phase is nearly parallel to the  $b_1$  slip direction in  $\beta$  phase, while there exists a significant ( $11.5^\circ$  about  $[0001]$ ) misalignment between the  $a_2$  slip direction in  $\alpha$  phase and the  $b_2$  slip direction in  $\beta$  phase. Hence, a thin  $\beta$  layer present between

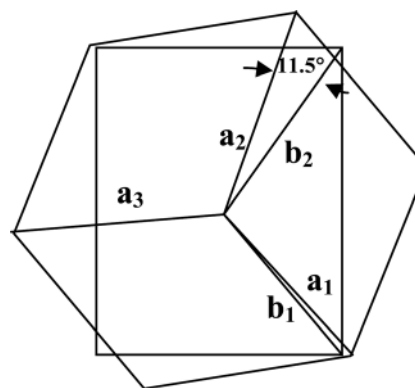


FIG. 15. Schematic representation showing orientation of slip direction in  $\alpha$  and  $\beta$  phase.

$\alpha$  laths can produce high resistance to the dislocation displacement and depending upon the wave propagation directions a colony of laths can contribute less toward harmonics generation. This is reflected in very low values of measured NLU parameter in some locations in furnace cooled structure and contributes to the scatter.

### C. Effect of interface dislocation

Besides dislocations inside the  $\alpha$  laths, interface dislocations also contribute to harmonics generation. Therefore, as the microstructure becomes finer as a result of higher cooling rate, the area fraction of interface increases resulting in increasing contribution of interface dislocation toward NLU parameter. It is to be noted that displacement of interface misfit dislocation depends upon mis-orientation across the lath interface. Misfit dislocations across high mis-orientation interface experiences high resistance in vibration and contribute little toward harmonics generation. Presence of a thin layer of stable  $\beta$  in the lath interface further produces high resistance to the dislocation displacement and corresponding decrease in the NLU parameter.

### D. Contribution of individual lath

In addition to the orientation factor contribution of individual laths toward harmonics generation depends upon: (1) dislocation density inside laths, (2) resistance to dislocation displacement for a given stress, (3) dislocation loop length, and (4) line direction or orientation of dislocation.<sup>17</sup> It is observed that dislocation density increases with increasing cooling rate (Fig. 14). As the dislocation density increases, the number of dislocation that vibrates under the action of oscillating stress also increases. It leads to increase in the amplitude of harmonics and increase in NLU parameter. On the other hand, higher dislocation density implies decrease in dislocation loop length that results in a decrease in the amplitude of vibration. This will reduce the amplitude of harmonics generation and thereby decrease in the NLU parameter.

### E. Combinational effect of different features on harmonics generation

As the degree of crystallographic orientation varies, randomness of the orientation of the slip systems in the

polycrystalline aggregates varies with respect to the wave propagation directions. This influences the NLU measurements to a large extent and scatter in the measurements largely varies depending upon the scale of crystallographic orientation change. In case of furnace cooled colony structure with laths oriented in a particular crystallographic direction within a  $\alpha$  colony, all the laths in the colony contribute simultaneously toward harmonics generation, dislocation displacement across colony produces relatively large amplitude of harmonics. In an extreme case of colony orientation along high symmetric wave propagation directions, amplitude of harmonics produced will be very high. Probability of recording these very high values during measurements at different locations depends upon the probability of colonies orientated along the high symmetric wave propagation directions. For other orientations amplitude of harmonics will decrease. Measurements done at several locations lead to variation in colony orientations, and thus, R will take a range of different values (but will remain constant for a slip system across the laths in a colony) that will get manifested as scatter in measurements. Apart from this, fairly coarse colony size (150–250  $\mu\text{m}$ ) leads to variation in crystallographic orientation at microscopic length scale. This results in significant variation in the interaction of ultrasonic wave with the insonified volume. Presence of a thin, continuous layer of  $\beta$  between the  $\alpha$  laths can cause further anisotropy in harmonics generation and contributes to the high scatter (as discussed in Sec. V B).

Possibility of such anisotropy does not exist in the rapidly cooled structures where the orientation of  $\alpha$  changes randomly over small length scales and continuous  $\beta$  layer is almost absent. Randomness of slip systems with respect to the wave propagation directions leads to incoherent interference of different rays. Measurements at different locations become equivalent with respect to the random lath orientations vis-à-vis wave propagation directions. Hence, with increase in cooling rate as randomness of the structure increases standard deviation systematically decreases. Thus, large scatter in NLU measurements has a strong correlation with the scale of crystallographic orientation change. The scale of crystallographic orientation change, which in turn, is governed by the colony size, dictates the nature of scatter in measurements. This is manifested through the plot of colony size versus standard deviation (Fig. 6). It is evident that a linear correlation exists between colony size and recorded standard deviation values. Further, the positively skewed frequency distribution with a very few recorded high value of NLU parameter for furnace cooled structure suggests the presence of relatively less high symmetric directions with few independent slip systems in the present alloy. This is consistent with the fact that the number of independent slip system will be 2, if  $(10\bar{1}0)$   $[11\bar{2}0]$  slip systems are assumed to be operative.

The overall trend of the average value of NLU parameter though suggests that several factors such as dislocation density inside laths, volume fraction of interface, change in the internal stress in side laths, interface dislocation vibration, etc., simultaneously contribute toward harmonics generation, but their contribution is largely dependent and

dominated by the scale of orientation change across colony/laths. Present study thus, establishes that NLU is a highly sensitive technique as compared to linear ultrasonic technique for determination of microstructural state of materials. This technique can be effectively used for the nondestructive characterization of micro-structural features for realization of desired mechanical properties during processing and to predict the state of damage in in-service components. At the same time, presence of local anisotropy in material can lead to anisotropy in harmonics generation and thereby considerable scatter in the measurements. The revelation of the present study thus, evokes serious implications to measurements of NLU parameter that has to be accounted during interpretation of results for assessment of microstructure in polycrystalline materials. A methodology consists of several measurements has to be adopted for proper interpretation of NLU results. This is important as change in microstructural state of materials associated with processing and in-service damages leads to evolution of preferred crystallographic orientation of different degree.

## VI. CONCLUSION

- (1) The physical basis of an unprecedented trend in “scatter” during measurement of NLU parameter has been explained using a dislocation string vibration model for harmonics generation for polycrystalline aggregates having variation in crystallographic misorientation at microscopic length scale.
- (2) Notwithstanding the experimental uncertainties in measurements, the present study conclusively establishes that the degree of “scatter” depends strongly on the scale and nature of the crystal orientation change and associated microstructural in-homogeneities. This has serious technological implications to interpretation of results of NLU study for assessment of microstructure.
- (3) Frequency distribution analysis of observed “scatter” values of the NLU parameter indicated a definite trend. It is shown that the characteristic of the distribution changes with variation in the colony size, crystalline symmetry and presence of stable beta in the alloy and a linear correlation exists between colony sizes and standard deviation of scatter values.
- (4) The general applicability of frequency distribution analysis for textured and non-textured material has been highlighted with an emphasis on NLU measurement methodology which calls for several measurements per specimen for microstructural correlation. The average value of NLU parameter obtained with limited measurements has limitations and can even lead to erroneous correlation of microstructural state with NLU parameter.

## ACKNOWLEDGMENTS

The authors wish to acknowledge the financial support from Defense Research and Development Organization, Government of India. The support rendered by the members of MEG, TAG, and NDTG of DMRL is gratefully acknowledged. Authors are grateful to Shri. Chandan Mondal, scientist, DMRL for stimulating discussions.

- <sup>1</sup>M. A. Breazeale and D. O. Thompson, *Appl. Phys. Lett.* **3**, 77 (1963).
- <sup>2</sup>R. D. Peters and M. A. Breazeale, *Appl. Phys. Lett.* **12**, 106 (1968).
- <sup>3</sup>D. C. Hurley, D. Balzar, P. T. Purtscher, and K. W. Hollman, *J. Appl. Phys.* **83**, 4584 (1998).
- <sup>4</sup>P. Li, W. T. Yost, J. H. Cantrell and K. Salama, IEEE Ultrasonics Symp., **1**, 1113 (1985).
- <sup>5</sup>J. H. Cantrell and W. T. Yost, *Appl. Phys. Lett.* **77**, 1952 (2000).
- <sup>6</sup>C. Mondal, A. Mukhopadhyay, and R. Sarkar, *J. Appl. Phys.* **108**, 4584 (2010).
- <sup>7</sup>J. H. Cantrell and W. T. Yost, *Int. J. Fatigue* **23**, 487 (2001).
- <sup>8</sup>S. P. Sagar, S. Das, N. Parida and D. K. Bhattacharya, *Scripta. Mater.* **55**, 199 (2006).
- <sup>9</sup>V. V. S. Jaya Rao, E. Kannan, R. V. Prakash, and K. Balasubramaniam, *J. Appl. Phys.*, **104**, 123508 (2008).
- <sup>10</sup>J. Kang, Q. Jianmin, A. Saxena, and L. Jacobs, edited by D. Thomson, and D. E. Chimenti, *AIP Conf. Proc.* **23**, 1248 (2004).
- <sup>11</sup>S. Baby, B. Nagaraja Kowmudi, C. M. Omprakash, D. V. V. Satyanarayana, K. Balasubramaniam, and K. Vikas, *Scripta. Mater.* **59**, 818 (2008).
- <sup>12</sup>J. S. Valluri, K. Balasubramaniam, and R. V. Prakash, *Acta Mater.* **58**(6), 2079 (2010).
- <sup>13</sup>L. Sun, S. S. Kulkarni, S. Krishnaswamy and J. D. Achenbach, *J. Acoust. Soc. Am.* **120** (5), 2500 (2006).
- <sup>14</sup>W. G. Burgers, *Physica* **1**, 561 (1934).
- <sup>15</sup>J. B. Newkirk and A. H. Geisler, *Acta Metall.* **1**, 370 (1953).
- <sup>16</sup>R. N. Thurston and M. J. Shapiro, *Acoust. Soc. Am.* **41**, 1112 (1967).
- <sup>17</sup>A. Hikata and C. Elbaum, *Phys. Rev.* **144**, 469 (1966).
- <sup>18</sup>A. Granato and K. Lüke, *J. Appl. Phys.* **27**, 583 (1956).
- <sup>19</sup>W. T. Yost and J. H. Cantrell, *Appl. Phys. Lett.* **94**, 021905 (2009).
- <sup>20</sup>J. H. Cantrell, *J. Appl. Phys.* **105**, 043520 (2009).
- <sup>21</sup>S. Suri, G. B. Viswanathan, T. Neeraj, D. H. Hou and M. J. Mills, *Acta Mater.* **47**, 1019 (1999).